ELSEVIER

Surface and Coatings Technology 116–119 (1999) 347–351

SURFACE & COATINGS TECHNOLOGY

www.elsevier.nl/locate/surfcoat

Nitriding of H-12 tool steel by direct-current and pulsed plasmas

E.J. Miola [a], S.D. de Souza [b], M. Olzon-Dionysio [b], D. Spinelli [a], C.A. dos Santos [c,*]

[a] *Departamento de Materiais, EESC–USP, 13560-250 São Carlos SP, Brazil*
[b] *Departamento de Física — UFSCar, 13565-950 São Carlos SP, Brazil*
[c] *Instituto de Física — UFRGS, C.P. 15051, 91501-970 Porto Alegre RS, Brazil*

Abstract

Direct-current (DC) and pulsed plasmas were used to nitride samples of AISI H-12 tool steel with treatment time varying from 1 h to 6 h. X-ray diffraction (glancing-angle and θ–2θ geometry), conversion electron Mössbauer spectroscopy, conversion X-ray Mössbauer spectroscopy and Vickers microhardness were used as analytical techniques. The near-surface compound layer consists of a mixture of γ'-Fe_4N and ϵ-$Fe_x(N,C)$, while the near-diffusion zone compound layer consists of a mixture of γ'-Fe_4N, ϵ-$Fe_x(N,C)$, α''-$Fe_{16}N_2$ and γ-austenite. For a DC plasma the dependence of compound layer thickness on nitriding time obeys a parabolic law, but for a pulsed plasma this dependence does not follow a parabolic law.

Keywords: H-12 tool steel; Microhardness; Mössbauer spectroscopy; Plasma nitriding; X-ray diffraction

1. Introduction

Several nitriding techniques have been used for a long time in industry to improve the tribomechanical properties of engineering components [1–3]. The tribomechanical properties of the treated materials are strongly related to the nature and size of the precipitates formed during the treatment, as well as their evolution when they are submitted to heating and/or stresses during work. The near-surface compound layer of plasma-nitrided steels consists mainly of ϵ-carbonitrides and γ'-Fe_4N nitride. The ϵ-carbonitride compounds comprise $Fe_2(N,C)$, $Fe_{3.2}(N,C)$ and $Fe_x(N,C)$, with $2<x<3.2$; hereafter referred to as ϵ_2, ϵ_3 and ϵ_x, respectively. Below this compound layer there is the so-called diffusion zone, α', where the steel matrix is supersaturated by the in-diffusion nitrogen. As a whole, the thickness of the compound plus diffusion zone correlates very well with the cross-sectional microhardness profile.

Significant data relating tribomechanical properties and nitriding parameters have been published in the past. However, this trend has not been followed by systematic studies related to the physico-chemical state of the nitrided steels. As a contribution to this subject we report an investigation on plasma-nitrided AISI H-12 tool steel, by comparing the effect of direct-current (DC) and pulsed glow-discharge plasmas on the physico-chemical state and kinetics of compound layer growth.

2. Experimental details

Mechanically polished samples of AISI H-12 tool steel [composition (wt%): 0.36 C, 0.87 Si, 0.43 Mn, 5.04 Cr, 1.73 Mo, 0.33 V and 1.14 W] were nitrided in an equipment similar to one described by Hudis [4]. The heat treatment before nitriding was: (1) austenitizing at 1293 K in air, for 30 min, followed by oil quenching; and (2) double tempering at 823 K in air, for 1 h, followed by air cooling. The Mössbauer spectrum of the sample after the heat treatment showed no signal of retained austenite. A mixture of H_2/20% N_2 under a total pressure of 0.6 kPa was used for all samples. Voltage and current density were adjusted to maintain the cathode temperature at 773 K. The temperature was measured by a chromel–alumel thermocouple embedded in a control sample. Two operational modes were used: (1) conventional DC voltage applied between the workpiece and the wall of the furnace, hereafter called DC glow discharge (DGD); and (2) pulsed voltage, operat-

* Corresponding author. Tel.: +55-31-316-6424; fax: +55-31-319-1762.
E-mail address: cas@if.ufrgs.br (C.A. dos Santos)

0257-8972/99/$ – see front matter
PII: S0257-8972(99)00207-8

ing at 9.83 kHz, referred to in the following as pulsed glow discharge (PGD). After nitriding for a time between 1 h and 6 h, the samples were submitted to slow cooling under vacuum inside the treatment chamber.

Cross-sectional microhardness profiles were obtained on mirror-polished surfaces etched with Nital 2% with a Zeiss microhardness tester equipped with a Vickers indenter, by using 0.07 kg load. X-ray diffraction patterns were acquired in θ–2θ geometry (XRD) and glancing-angle geometry (GXRD) by means of a Siemens diffractometer, equipped with a curved graphite monochromator and Cu Kα radiation ($\lambda = 0.1542$ nm). XRD measurements were done with a scan step of $2\theta = 0.05^\circ$ in the 2θ range from 10° to 80°, with a fixed counting time of 1 s, while GXRD patterns were obtained with incidence angle fixed at 3°, scan step of $2\theta = 0.02^\circ$ and counting time of 4 s. For this incidence angle, the layer thickness probed by X-rays is about the same as that probed by the conversion electron Mössbauer spectroscopy (CEMS) technique ($\cong 0.2$ μm). The Mössbauer spectroscopy data were obtained in a backscattering geometry. A proportional counter with He–5% CH_4 (for CEMS) or Ar–5% CH_4 [for conversion X-ray Mössbauer spectroscopy (CXMS)] was added to a conventional, constant-acceleration Mössbauer spectrometer. The source was ^{57}Co in a rhodium matrix with a nominal activity of 25 mCi. All the CEMS and CXMS measurements were performed at room temperature (RT). Isomer shifts are given relative to α-Fe at RT.

3. Results and discussion

Fig. 1 shows XRD patterns for the samples nitrided for 1 h and 3 h, using PGD [Figs. 1(a) and (b)] and DGD [Figs. 1(c) and (d)] processes. There is no evidence of martensitic reflections from the steel matrix, even for the smallest nitriding time. Therefore, we conclude that the effective thickness of the compound layer is larger than the effective range probed by the Cu Kα radiation [5], roughly 10 μm. The compound layer comprises essentially ϵ-Fe_{2-3}(C,N) and γ'-Fe_4N. For the DGD process, the ϵ-carbonitride layer is highly textured along the $\langle 101 \rangle$ direction for the sample nitrided for 1 h, but shows a clear polycrystalline character for increasing nitriding time. For the DGD process, the γ' reflections are virtually absent from the XRD pattern of the sample nitrided for 1 h [Fig. 1(c)] and grow monotonically with increasing nitriding time [Fig. 1(d)]. Therefore, at the initial step of the nitriding process, the contribution from the γ' component is more significant for PGD samples than for DGD ones. However, XRD and GXRD measurements show clearly that the situation is reversed after 4 h.

The CEMS spectrum for the as-received sample confirms the XRD measurements as the hyperfine parameters can be attributed to α'-(Fe,C,N) martensite [6]. Fig. 2 displays CEMS spectra of the samples for which the XRD patterns are shown in Fig. 1. These spectra were fitted by the addition of sub-spectra corresponding to α', γ', ϵ_3 and ϵ_x, with typical hyperfine parameters as displayed in Table 1, which are quite similar to those previously published [6–11]. The CEMS spectrum for the PGD sample nitrided for 1 h [see Fig. 2(a)] consists of 31% α', 20% γ', 33% ϵ_3 and 16% ϵ_x. For nitriding time $t \geq 2$ h, all the CEMS spectra are quite similar for both processes. Minor differences, as reflected by the relative spectral areas, can only be discriminated by the fitting procedures.

These trends are also observed for the CXMS measurements, as can be seen in Table 2. As an illustration, Fig. 3 displays the CXMS results obtained for the samples discussed above. We observe that, within the experimental resolution, the CXMS spectra for the sample nitrided for 1 h [Figs. 3(a) and (c)] are largely process-dependent. On the other hand, the CXMS

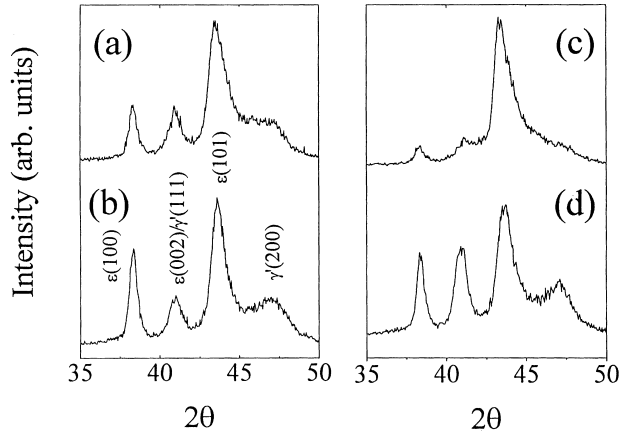

Fig. 1. θ–2θ X-ray diffractograms for: PGD samples nitrided for 1 h (a) and 3 h (b); DGD samples nitrided for 1 h (c) and 3 h (d).

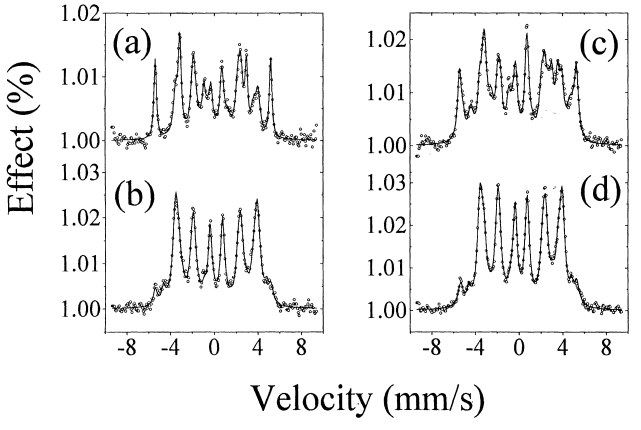

Fig. 2. CEMS spectra for the same samples described in Fig. 1. The solid lines are fitted spectra, as described in the text.

Table 1
Typical values of the parameters used to fit the different ^{57}Fe CEMS and CXMS spectra shown in this work. The isomer shifts are given relative to α-Fe. Typical errors are ±3%

Component	H (kG)	ΔE_Q (mm s^{-1})	d (mm s^{-1})
α′-martensite	331	0.01	0.01
γ-(Fe−N−C) austenite	–	–	−0.12
	–	0.32	0.05
α″-$Fe_{16}N_2$	314	0.09	0.17
ε-$Fe_{3.2}$(C,N)	290	0.02	0.29
	241	0.02	0.32
ε-Fe_{2+x}(C,N), $x<1.2$	220	0.03	0.32
	108	0.01	0.51
	–	0.95	0.45
γ′-Fe_4N	338	0.02	0.25
	210	0.25	0.32

Table 2
Relative CEMS and CXMS spectral areas for samples nitrided under the DGD condition. Typical errors are ±5%

Nitriding time (h)	CEMS/CXMS					
	α′	α″	γ	γ′	$\epsilon_{3.2}$	ϵ_x ($x<3.2$)
1	30/49	0/13	0/5	30/4	33/19	8/10
2	14/–	0/–	0/–	23/–	54/–	9/–
3	12/42	0/6	0/0	25/12	54/34	9/7
5	–/42	–/8	–/3	–/13	–/29	–/5
6	7/–	0/–	0/–	35/–	51/–	7/–

spectra for the sample nitrided for 3 h [Figs. 3(b) and (d)] are quite similar. A general outlook of evolution of the compound layer can be obtained from Tables 2 and 3.

Fig. 4 shows the CEMS and CXMS ϵ/γ' spectral area ratios as a function of the nitriding time, for DGD and PGD processes. For all cases the ϵ/γ' spectral area ratios are larger than 1. This result would be expected, since we are using a nitriding atmosphere at proportion $N_2/H_2=1/4$ [2]. The near-surface evolution, as viewed by CEMS measurements (probed range ≈0.2 μm), are

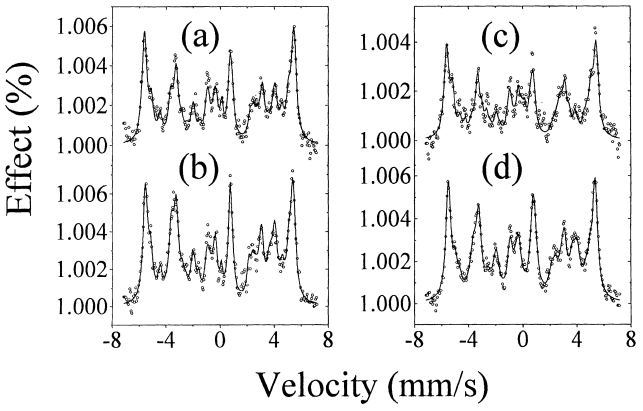

Fig. 3. CXMS spectra for the same samples described in Fig. 1. The solid lines are fitted spectra, as described in the text.

Table 3
Relative CEMS and CXMS spectral areas for samples nitrided under PGD conditions. Typical errors are ±5%

Nitriding time (h)	CEMS/CXMS					
	α′	α″	γ	γ′	$\epsilon_{3.2}$	ϵ_x ($x<3.2$)
1	31/48	0/10	0/4	20/7	33/26	16/5
2	10/–	0/–	0/–	19/–	64/–	7/–
3	7/40	0/9	0/2	21/7	66/35	6/7
5	–/40	–/10	–/2	–/11	–/33	–/4
6	5/–	0/–	0/–	24/–	61/–	11/–

quite similar but, consistent with the XRD results, the ϵ/γ' ratio is invariably larger for the PGD process. As the nitriding time increases from 1 to 2 h the thickness of the ϵ layer increases, compared with the γ' layer. For $t>2$ h, the ϵ/γ' ratio decreases monotonically. This is consistent with relative growth of the γ' layer near the surface as the nitriding time increases. At a deeper layer, as viewed by CXMS measurements (probed range ≈2 μm), the behaviour is process-dependent. When the nitriding time increases from $t=1$ h to $t=3$ h, the γ' layer increases for the DGD process and decreases for the PGD one. For $t>3$ h the γ' layer increases for both processes.

The carbon present in the steel matrix, in addition to its increased concentration due to treatment contamination, could induce θ-Fe_3C precipitation. We have tried to use the parameters from this phase [12] in our fitting scheme to the CXMS spectra, but they were unequivocally ruled out. On the other hand, as expected, α″-$Fe_{16}N_2$ precipitation was observed on the CXMS spectra as a consequence of the slow cooling. CXMS measurements have also suggested the existence of minor amounts of γ-austenite near the diffusion zone (see

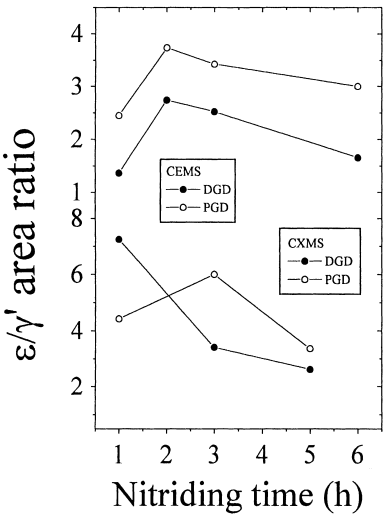

Fig. 4. ϵ/γ' relative spectral area ratio obtained from the CEMS and CXMS spectra. Solid symbols refer to DGD samples and open symbols to PGD samples. The solid lines are a guide for the eye.

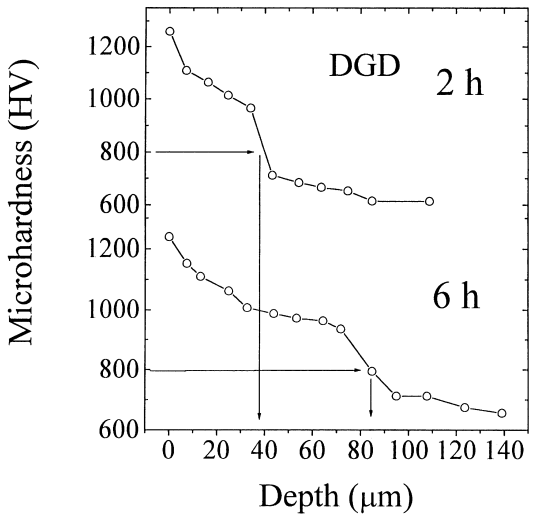

Fig. 5. Vickers microhardness profiles as a function of depth from the nitrided surface for DGD samples nitrided for 2 h and 6 h.

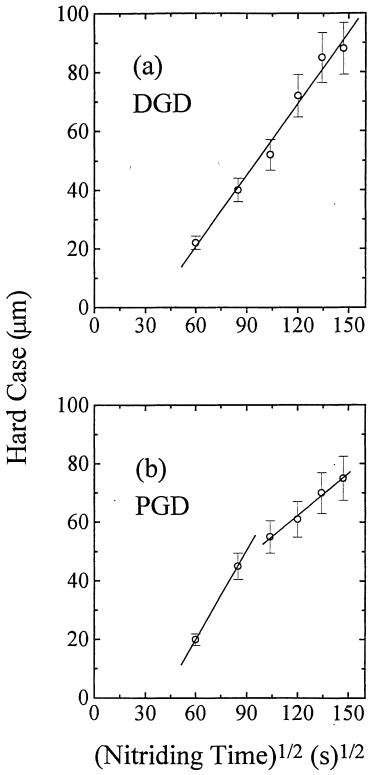

Fig. 6. Thickness of the hardest layers as a function of square root of the nitriding time for (a) DGD and (b) PGD samples.

Tables 2 and 3). The quadrupolar doublet present in the CXMS spectra (see Table 1) have been observed in iron submitted to successive implantation of nitrogen and carbon, but was not attributed to any known nitride or carbide [13]. We propose now that this doublet, and the singlet with $\delta_{Fe} = -0.12\ mm\ s^{-1}$, be attributed to γ-austenite containing carbon and nitrogen.

Vickers microhardness profiles as a function of depth from the nitrided surface are depicted in Fig. 5 for DGD samples nitrided for 2 h and 6 h. The thickness of the hard layers can be estimated from the microhardness profiles by arbitrarily assuming 800 HV as the minimum hardness of the nitrided layer (the hardness of tempered H-12 steel, before nitriding, is 600 ± 50 HV). As illustrated in Fig. 5, the thickness of the hard layers is about 38 μm for the DGD sample nitrided for 2 h and about 85 μm for that nitrided for 6 h. The thickness of the hardest layers as a function of the square root of the nitriding time, shown in Fig. 6, represents the kinetics of the compound layer growth for DGD and PGD samples. The DGD curve, Fig. 6(a), obeys a parabolic law, although a tendency for saturation is suggested for nitriding time $t > 5$ h. The PGD curve, Fig. 6(b), clearly deviates from the parabolic law. It appears that the compound layer for PGD samples grows in steps with different kinetics. At the initial stage ($t < 3$ h) the compound layer grows faster than at the final stage ($t > 2$ h). For PGD samples a tendency for saturation could be observed only for nitriding time $t > 6$ h. Similar results have been reported for several materials plasma-nitrided under different process parameters [14–18]. However, we do not have sufficient experimental data to support a clear explanation for such a behaviour.

4. Conclusions

A systematic investigation of the crystal and chemical state of the compound layer and cross-sectional microhardness profile was undertaken on AISI H-12 tool steel treated by DC glow discharge (DGD) and by pulsed glow discharge (PGD). X-ray diffraction (XRD), conversion electron Mössbauer spectroscopy (CEMS), conversion X-ray Mössbauer spectroscopy (CXMS) and Vickers microhardness were used as analytical techniques. The results suggest that, under the present experimental conditions:

1. the near-surface compound layer, as probed by CEMS, consists of a mixture of γ′-Fe_4N and ϵ-$Fe_x(N,C)$;
2. the near-diffusion zone compound layer, as probed by CXMS, consists of a mixture of γ′-Fe_4N, ϵ-$Fe_x(N,C)$, α″-$Fe_{16}N_2$ and γ-austenite; and
3. the kinetic behaviour for DGD samples obeys the parabolic law, while that for PGD samples clearly violates the parabolic law. The latter grows with two different kinetics: faster at the initial stage ($t < 3$ h) and slower at the final one.

Acknowledgements

We are much indebted to Drs F.C. Zawislak and P.M. Mors for stimulating discussions. One of us (EM) acknowledges the hospitality of the IF-UFRGS staff

during his stay at Porto Alegre. This work was partly supported by the Brazilian agencies CAPES, CNPq/PRONEX, FINEP and FAPERGS.

References

[1] J.R. Conrad, J.L. Radtke, R.A. Dodd, R.J. Worzala, N.C. Tran, J. Appl. Phys. 62 (1987) 4591.
[2] Y. Sun, T. Bell, Mater. Sci. Eng. A 140 (1991) 419.
[3] G.A. Collins, R. Hutchings, J. Tendys, M. Samandi, Surf. Coat. Technol. 68/69 (1994) 285.
[4] M. Hudis, J. Appl. Phys. 44 (1973) 1489.
[5] R. Delhez, Th.H. de Keijser, E.J. Mittemeijer, Surf. Eng. 3 (1987) 331.
[6] N. DeCristofaro, R. Kaplow, Metall. Trans. A 8 (1977) 35.
[7] K.H. Eickel, W. Pitsch, Phys. Status Solidi 39 (1970) 121.
[8] A.J. Nozik, J.C. Wood Jr., G. Haacke, Solid State Commun. 8 (1970) 8.
[9] G. Le Caer, A. Simon, A. Lorenzo, J.M. Génin, Phys. Status Solidi A 6 (1971) K97.
[10] D. Firrao, M. Rosso, G. Principi, R. Frattini, J. Mater. Sci. 17 (1982) 1773.
[11] C.A. dos Santos, B.A.S. de Barros Jr., J.P. de Souza, I.J.R. Baumvol, Appl. Phys. Lett. 41 (1982) 237.
[12] M. Ron, Z. Mathalone, Phys. Rev. B 4 (1971) 774.
[13] C.A. dos Santos, I.J.R. Baumvol, E.A. Garcia, M. Behar, J. Phys. D: Appl. Phys. 17 (1984) 969.
[14] U. Figueroa, J. Oseguera, P.S. Schabes-Retchkiman, Surf. Coat. Technol. 86–87 (1996) 728.
[15] J.L. Albarran, J.A. Juárez-Islas, L. Martinez, Mater. Lett. 15 (1992) 68.
[16] J. D'Haen, C. Quasyhaegens, G. Knuyt, M.. D'Olieslaeger, L.M. Stals, Surf. Coat. Technol. 74 (1995) 405.
[17] V.I. Dimitrov, J. D'Haan, G. Knuyt, C. Quasyhaegens, L.M. Stals, Appl. Phys. A 63 (1996) 475.
[18] Y. Sun, T. Bell, Mater. Sci. Eng. A 224 (1997) 33.